Enhanced Raman forward scattering

D. L. Fisher and T. Tajima
Physics Department, University of Texas, Austin, Texas 78712
(Received 9 August 1995)

Recent experiments on laser wake-field acceleration have indicated a dramatically enhanced value of the accelerating field created through the process of the Raman forward scattering instability. However, the use of the Raman forward scattering instability can be improved. If the initial growth of the instability is from noise, its evolution has problems of reproducibility and is unpredictable in both time and space. We suggest the addition of a small amount of one of the scattered products to the laser pulse or plasma as a seed. This allows the instability to grow from a known and controllable source, giving predictable and reproducible results. Additionally, simulations show that the final wake field and pulse modulation occur much faster and are cleaner with a seed than without. Seeding is especially important when we are operating in the low plasma density or low laser pulse intensity regime. We discuss methods to produce a seed and applications for the production of short laser pulses and electron bunches by this process.

PACS number(s): 52.75.Di, 52.40.Nk

I. INTRODUCTION

A recent experiment [1] dramatically indicates an important role that the Raman forward scattering (RFS) instability plays to induce the plasma wave and to accelerate electrons in a laser-pulse-induced plasma wake field [2,3]. Previous to this experiment, it has been suggested that the RFS may be used to drive an accelerator [4–6]. Thus the instability allows a certain amount of laser pulse length detuning from the resonant pulse length, and the instability can induce the plasma self-organization to form the correct modulation of the laser pulse and wavelength of plasma oscillations. This is exciting because the plasma and its instability act resonantly (nearly) regardless of the precise conditions of the laser and plasma. Earlier, this instability was observed to generate superhot electrons [4]. There are at the present time a number of planned and ongoing laser wake-field experiments in both the linear and RFS regimes.

In this paper we consider the one dimensional self-modulation of a laser pulse by stimulated Raman forward scattering. Techniques to enhance the amplitude of the one-dimensional Raman forward self-modulation and to reduce the time for this instability to grow are investigated. Also, applications for the production of ultrashort (≈ 1 fs) laser and electron pulses are discussed. When this modulation process goes to completion, we observe that the laser pulse forms a trains of ultrashort pulses, which may be separated and used for other applications. Also, since the plasma wavelength is short, ultrashort buckets of accelerated electrons from the plasma (or from injected longer bunches which are bunched into shorter bunches) may also be separated and used for various applications.

The enhancement techniques fall into two categories. The first is Raman seeding, where the main high intensity laser pulse is mixed with a low level intensity seed pulse. The second is plasmon seeding, where the initial plasma oscillations is induced by some method so that the initial plasma oscillations do not have to grow from noise.

II. THEORY

Scattering of large amplitude light (primary radiation) in a plasma into a plasmon and a scattered photon is known as stimulated Raman scattering [7]. If the scattered radiation is in the direction of the original light (Raman forward scattering), it will copropagate and beat with the original light, thereby modulating the laser pulse. This modulation reinforces and amplifies the plasma oscillation, increasing the growth of the scattered radiation. This is known as the Raman instability.

When the first Raman forward shift ($k_{\text{Raman}} = k_0 \pm k_p$) beats with the original laser pulse, it produces an amplitude modulation with spacing $2\lambda_p$ on the original laser field. The modulation of the intensity and E^2 has a spacing of λ_p, which is then resonance with the plasma oscillation. However, the higher order Raman forward shifts ($\pm 2k_p, \pm 3k_p, \ldots$) beat with the original radiation to form an intensity of E^2 modulation spacing of $(\lambda/2, \lambda/3)\ldots$, which are not resonance with the wake field. These higher order nonresonances will degrade the amplitude and clarity of the wake field.

The growth of any order for simple Raman forward scattering (SRFS) depends upon the amount of energy in that order, in the source order, and in the plasma oscillation. That is, energy flows from zeroth to first to second, etc. [8]. Due to this last factor and the variation of the amplitude of the plasma oscillation, the Raman dynamics which takes place in a long laser pulse ($l_p \gg \lambda_p$) may vary considerably within that laser pulse. This variation in Raman dynamics is due to the amplification of the plasma oscillation within the laser pulse as the wave travel toward the rear of that laser pulse. This amplification, as described above, is due to the resonance structure of the modulated laser pulse. Since the amplitude of the

 ©1996 The American Physical Society

laser pulse is larger as you approach the rear of the laser pulse (until higher order shifts build up there), Raman forward scattering is greater in this region, and the amount of Raman energy is largest toward the tail of the laser pulse. However, as the second and higher order Raman shifts build up in these regions of the laser pulse, they start to form nonresonance structures which degrade the wake field.

The time (length) it takes for SRFS to modulate the pulse to an appreciable level depends on several factors. The first is the intensity of the primary (original) radiation; the more intense this is (the more photons per unit volume), the greater the amount of radiation scattered. The second is the density of the scattered photons and plasmons, again as expected; the greater the density, the more scattered products occur (the inverse process will have a small cross section since the plasmons are left behind). If there is no initial seeding, the scattered products must grow from noise. The plasmon noise is generally induced by the laser pulse itself, through a number of possible mechanisms to be described below.

If the primary pulse is of low intensity, the time (interaction length) it takes for self-modulation to occur may be long. This time may be greatly reduced by seeding the scattered photons, plasmons, or both. The process of seeding is approximately equivalent to an unseeded pulse interaction with the plasma over the length it takes to RFS the equivalent amount of energy that is in the seed. However, there are several important differences. The differences depend upon the method used to produce the seed. The first is where the energy is deposited in the laser pulse. With most seeding processes, we are able to distribute the seed energy in any manner we wish within the laser pulse (perhaps evenly distributed or most at the initial part of the laser pulse). The second is the ability to produce a seed without higher or other unwanted Raman orders. Even if they are produced, they may be removed with a filter. The ability to manipulate the seed in this manner is the reason for a cleaner, predictable, and reproducible wake field. Seeding is also particularly important in regimes where the grown rate is low. These are in the low density and/or low intensity regimes, or where the interaction length is short.

Initial plasma oscillation noise may originate from at least four sources. The first is from the ponderomotive force of the laser. However, if the laser pulse is a long way from resonance (for resonance $l_{\text{laser}} < \lambda_p$), the plasma oscillation is small. The next source of noise is due to the ionization front. There are two factors here; the first is the plasma oscillation caused by the plasma pressure force whose peak amplitude is proportional to the plasma temperature [see Sec. III, Eq. (8)]. The second noise source due to an ionization front is from the depletion of laser pulse energy in the region of the ionization front [9]. When the plasma is suddenly formed in the laser pulse, there is a loss of energy by the laser pulse in the region of ionization. This depletion of the laser pulse causes a sharp spike, which gives a ponderomotive kick to the plasma oscillation. This induces a larger plasma oscillation than the smooth laser pulse would produce. The third source is laser pulse energy depletion due to Raman backscattering, which has an abrupt transition to turn on. This, as in ionization depletion, forms a sharp leading edge or a spike in the laser pulse, which again gives a ponderomotive kick to the plasma oscillation. The fourth is from noise due to the plasma distribution of thermal velocity or temperature. The lowest estimate of the electric field may be evaluated using the fluctuation-dissipation theorem [see Sec. III, Eq. (21)]. Simulations described in Sec. IV do not include the ionization effects. However, they do include the other effects of the envelope and Raman backscattering, as described above.

In addition to the one-dimensional Raman forward scattering, there is also a competing two-dimensional Raman scattering [10], sometimes called self-modulation. This two-dimensional Raman scattering also modulates the laser pulse in a resonant manner with the wake field. The growth rate for Raman forward scattering exceeds that for self-modulation [10] when $k_p r_0 > \omega_0/\omega_p$, where r_0 is the spot size of the laser pulse. It should also be noted that seeding for Raman forward scattering will also decrease the time for pulse modulation even in the two-dimensional regime.

III. IONIZATION-INDUCED WAKE FIELDS

In this section we investigate an effect associated with the production of a wake field. An intense laser pulse (or charged particle beams) quickly ionizes the gas at or near the front of the pulse, and thereby set up an ionization front. This we find carries a chemical potential, which can be applied to particle accelerators. This ionization of the gas (or metal) produces a density gradient in the ionization front, and this may be seen as a pressure force in the moving frame of the front. This force will induce a plasma oscillation in its wake whose phase velocity is equal to the velocity of the ionization front, which for a laser or relativistic particle beam is approximately equal to c. The wake field induced by the ionization front may be used as the plasmon noise source for laser pulse self-modulation and wake-field production by stimulated Raman forward scattering.

To investigate the wake field induced for a short ($\tau_i \ll \tau_p$) ionization front with nonrelativistic thermal velocities analytically, we employ a linear two-dimensional fluid model with axial symmetry. We model the ionization front as a thermal pressure force $[F_p = Te\nabla n_{iz}(r,z,t)]$ in the momentum equation with the ions fixed. We also assume the thermal velocities have a Maxwellian distribution. For the momentum equation this gives

$$m\frac{\partial \vec{v}}{\partial t} = \vec{\nabla}\left[e\phi + \frac{T_e}{n_0 c} n_{iz}(r,z,t,\right] . \tag{1}$$

The linearized continuity and Poisson's equations are

$$\frac{\partial n}{\partial t} + n_0 \vec{\nabla}\cdot\vec{v} = 0 , \tag{2}$$

$$\nabla^2\phi = 4\pi e n , \tag{3}$$

where n is the electron charge density, ϕ is the electric

wake-field potential, T_e is the electron temperature, and n_{iz} is the ionization front density profile. Here we will assume the ionization process has no effect on the ionizing agent, and that there is no time dependence in the moving frame. This moving frame travels at the speed of light c, approximately the speed of the ionizing agent. With these assumptions, we make the change of variables to $\lambda = t - z/c, r$, and from Eqs. (1)–(3) yields

$$\frac{\partial^2 \phi}{\partial \lambda^2} + \omega_p^2 \phi = -\omega_p^2 \frac{T_e n_{iz}(r,\lambda)}{e n_0 c} . \tag{4}$$

Solving for ϕ gives

$$\phi(r,\lambda) = \omega_p \int_{-\infty}^{\lambda} d\lambda' \sin[\omega_p(\lambda - \lambda')] \frac{T_e n_{iz}(r,\lambda')}{e n_0} . \tag{5}$$

For our short ionization front ($\tau_i \ll \tau_p$), we use the ionization profile

$$n_{iz} = \frac{n_0}{\omega_p} e^{-r^2/2\sigma_r^2} \delta(\lambda) . \tag{6}$$

Substitution of Eq. (6) into Eq. (5) yields, for the longitudinal field,

$$E_z = \omega_p \frac{T_e}{ec} \cos(\omega_p \lambda) e^{-r^2/2\sigma_r^2} , \tag{7}$$

and for the peak axial longitudinal field,

$$E_{\text{peak}} = \omega_p \frac{T_e}{ec} . \tag{8}$$

Now we will numerically investigate this phenomenon using a two dimensional nonlinear fluid model with axial symmetry, and, as previously, the ionization front is modeled as the force due to the density gradient produced by the ionization front. This formalism is not self-consistent in that the ionizating agent (or any agent causing the force term in the momentum equation) does not evolve in time. This is valid if the agent causing the force does not change significantly over the time of interest. The relativistic equation of motion is

$$\frac{\partial \vec{p}}{\partial t} + (\vec{v}\cdot\vec{\nabla})\vec{p} = -e\left[\vec{E}_e + \frac{1}{c}(\vec{v}\times\vec{B})\right] + \vec{F}_{nl} , \tag{9}$$

where F_{nl} can be ponderomotive or pressure force. For ionization $\vec{F}_{nl} = -\vec{\nabla} P_e$, where $P_e = T_e n$ is used since the thermal velocities of interest are nonrelativistic. This equation along with the continuity equation

$$\frac{\partial n}{\partial t} + \vec{\nabla}\cdot(n\vec{v}) = 0 , \tag{10}$$

and Maxwell's equations

$$\vec{\nabla}\times\vec{B} = \frac{4\pi}{c}\vec{j} + \frac{1}{c}\frac{\partial \vec{E}}{\partial t} , \tag{11}$$

$$\vec{\nabla}\times\vec{E} = -\frac{1}{c}\frac{\partial \vec{B}}{\partial t} , \tag{12}$$

where $\vec{j} = -en\vec{v}$ are used to formulate the fluid code. An axial symmetry is assumed, yielding

$$-\vec{\nabla}P_e = -T_{e_z}\frac{\partial n}{\partial z}\hat{z} - T_{e_r}\frac{\partial n}{\partial r}\hat{r} = F_z\hat{z} + F_r\hat{r} . \tag{13}$$

We look for a solution in the rest frame of the ionizing pulse with $v_g \simeq c$. Now, as before, we change variables to a one dimensional system $[r, t-(z/c) \equiv t]$. All quantities are considered fixed in the moving frame; that is, there is no time evolution in this moving frame. Only the azimuthal component of the magnetic field is nonzero due to symmetry. This code is described in [11], except for the origin of the nonlinear force. Results are given in Sec. IV.

Next we look at a comparison of the wakefields induced by the ponderomotive force of the laser to that of the ionization potential. The peak electric force due to the ionization potential is given by Eq. (8),

$$eE_i = \frac{\omega_p}{c} T_e , \tag{14}$$

and that due to the ponderomotive force for a resonant laser pulse is [2].

$$eE_p = \frac{\omega_p}{c} mc^2 \frac{I}{I_0} , \tag{15}$$

where I_0 is the intensity at $v_{\text{osc}} = c$.

Setting $E_i = E_p$, we obtain

$$T_e = mc^2 \frac{I}{I_0} = m v_{\text{osc}}^2 , \tag{16}$$

where

$$v_{\text{osc}} = \frac{eE_{\text{laser}}}{\omega m} \tag{17}$$

yielding $T_e = m(eE_{\text{laser}}/\omega m)^2$. The intensity is

$$I = \frac{cE_{\text{laser}}^2}{4\pi} = \frac{mc}{4\pi e^2}\omega^2 T_e , \tag{18}$$

which gives

$$[I(W/cm^2)] = \frac{5.3\times 10^{12}[T_e\ (\text{eV})]}{[\lambda_0^2(\mu\text{m})]^2} , \tag{19}$$

where λ_0 is the wavelength of the laser (in μm). At this power the ponderomotive and ionization potentials are equal. Below this power the ionization potential dominates, and above it the ponderomotive potential dominates.

Now we look at the level of noise due to the plasma thermal velocity. From the fluctuation-dissipation theorem, we know that the energy density of the k component of the noise due to the fluctuations at thermal equilibrium is given by

$$\langle E_{\text{noise}}^2(\vec{k})\rangle = 4\pi T_e . \tag{20}$$

Since we are interested in noise of wavelength about ω_p/c, this leads to

$$E_{\text{noise}} \simeq \left[\frac{\omega_p}{c}\right]^{3/2} \sqrt{4\pi T_e} . \tag{21}$$

Usually the level of the noise field is higher then this value.

IV. SIMULATION AND RESULTS

A. Ionization

The results of the one-dimensional kinetic simulations and the two-dimensional (axial symmetric) fluid simulations are compared to theory. The one-dimensional kinetic code is a fully relativistic electromagnetic particle-in-cell code with vacuum boundary conditions. The laser pulse amplitude is purposely set low ($u_{osc}/c=0.001$), so the only effect is due only to ionization and not due to the ponderomotive force. After a threshold is achieved, total ionization takes place in ionization time τ_i, which is set to a value much less than the plasma period. The wake field is insensitive to the value of the τ_i as long as the condition $\tau_i \ll \tau_p$, as predicted by the linear fluid analysis.

In Fig. 1 we show the results of both the kinetic and fluid runs [with large σ_r for one-dimensional (1D) results] by a Gaussian density thermal pressure for various electron temperatures. From this graph we see that the slope of the peak wakefield versus the electron temperature is unity, as predicted by the linear fluid model. In all the fluid runs (with large σ_r), the value of the peak wake field produced by the ionization front compared very well with the kinetic runs (see Fig. 1). Since the kinetic code actually models the ionization of the material (with a thermal profile), the consistent agreement of the results with those of the fluid code justifies our model for the ionization front as a pressure force. Using the nonrelativistic formulation of the force due to the pressure gradient is valid since, although the ionization front moves with velocity approximately equal to c, the velocity of the electrons in this front are at the thermal velocity. In all runs, nonrelativistic thermal velocities were used. With this model, the only effect of the ionizing agent (laser, charged particle beam, etc.) is through the pressure force term. This model does not include the effect of the ionization process other than the pressure force nor the plasma effects on the ionizing agent.

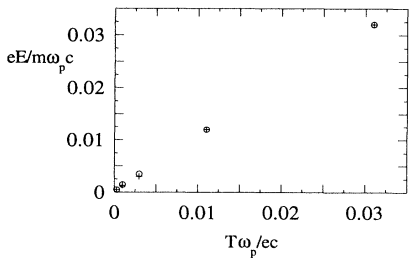

FIG. 1. Comparison of the results for the kinetic (+) and fluid (o) computer code runs for wake-field production by a Gaussian density thermal pressure at various temperatures. The note slope is equal to unity, the value predicted by the linear theory.

B. Raman forward scattering

Simulations of the one-dimensional SRFS regime were completed using a modified fully relativistic PIC (particle in cell) computer code. To reduce computer time and memory in long run simulations, we introduced a moving frame, which follows the laser pulse as it travels in the PIC code. In this modified code the time at which the moving code is engaged and the velocity that the frame moves are both controllable. This is to allow the laser pulse to move into the plasma from a vacuum, and then the moving frame is engaged. Also, there may be reasons to allow the moving frame to travel at some speed other than the speed of light (for example, $v_g < c$), so this is also adjustable. The moving frame works by moving each cell back one space when a proper number of time steps have occurred and adding plasma to the front of the plasma. Care must be taken to assure that the laser pulse and any changing quantities never make it to the front of the simulation box. Also, as the cell are retarded, the end cells are removed. It is to be mentioned that this is not a Lorentz transformation and only a Galilean transformation. The value of laser and plasma fields are, therefore, those in the nonmoving laboratory frame. Simulations were run with vacuum boundary conditions and 20 particles per cell. The laser pulse is initialized in vacuum, and then allowed to evolve into the plasma for more realistic initial conditions, and to reduce artificial growth of the SRFS from noise.

It is important in simulation of SRFS to make sure that the noise source for the SRFS originates only from true physical factors, and is not due to some numerical source or unphysical initial conditions. This is accomplished by varying simulation parameters and observing if any changes took place in the growth rate or results. One check is to vary the number of particles per cell, which we did using five, ten, and 20 particles per cell with no observed changes. Also, the leading edge of the laser pulse must be smooth with no abrupt starts as this will artificially seed the plasma oscillation. In our simulations the leading edge of the Gaussian laser pulse dropped smoothly over 10σ, leaving a very smooth leading edge.

C. Seeding

To investigate laser pulse seeding and shaping, we initially ran a reference simulation, which is an unseeded and unshaped (smooth Gaussian with $\sigma \gg \lambda_p$) laser pulse. We then demonstrate the effect that a sharp leading edge (plasmon seed) has on the evolution of that laser pulse. Existing pulse shaping techniques may be used to form this pulse [12,13]. Finally, the evolution of a laser pulse with a Raman intensity seed of 0.001 the intensity of that laser pulse is demonstrated.

The reference, to compare with the shaped and Raman seeded laser pulse simulations, is that of a low intensity laser pulse in a high density plasma. In Fig. 2(a) we show an unseeded Gaussian laser pulse which for a plasma density of 3×10^{19} cm^{-3} gives a peak laser pulse intensity of 2×10^{16} W/cm^2 with a pulse length of 100 fs. Figure 2(b) shows an unseeded laser pulse with a sharp leading edge.

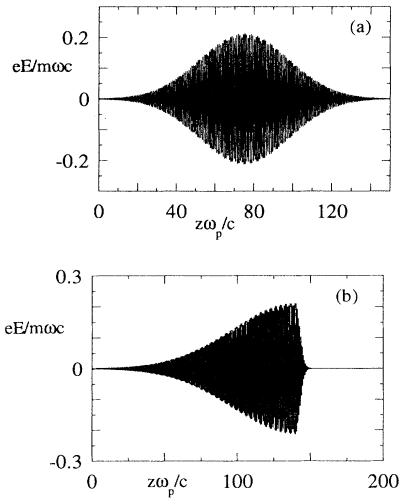

FIG. 2. (a) and (b) show the initial unseeded Gaussian and shaped laser pulses. The initial Raman seeded laser pulse is almost identical to the initial unseeded laser pulse.

The sharp leading edge induces a large initial plasma oscillations from which the SRFS will grow. This initial plasma oscillation is order of magnitudes larger than that for the unshaped laser pulse [Fig. 2(a)], and we consider this laser pulse, as its appearance is identical to Fig. 2(a) at this scale. This is due to the fact that the amount of Raman shifted energy in the seeded laser pulse is only 0.001 the energy of the unseeded laser pulse. The seeded energy is at the shifted wave number ($k_{\text{Raman}}=k_0-k_p$). Figures 3(a)–3(c) show the laser pulse after $\omega_p t=750$. There is very little modulation of the unseeded laser pulse [Fig. 3(a)] when compared to the modulation of the shaped laser pulse [Fig. 3(b)], and the seeded laser pulse [Fig. 3(c)]. This modulation is due to the larger amount of Raman shifted energy in the plasmon and Raman seeded laser pulse, which may be seen in the spectrum (Fig. 4). Figure 4 shows the wave-number spectrum of the laser pulse at $\omega_p t=750$. As expected from observations of the laser pulse, there is little Raman energy in the unseeded laser pulse [Fig. 4(a)]. However, the plasmon seeded [Fig. 4(b)] and Raman seeded [Fig. 4(c)] spectra show considerable conversion of laser energy to the Raman frequency. At this time, the first Raman shift dominates leaving a large clean wake field for the plasmon seeded [Fig. 5(b)] and Raman seeded [Fig. 5(c)] laser pulse. A comparison to the wake field of the unseeded [Fig. 5(a)] laser pulse demonstrates the advantage of seeding. Even at $\omega_p t=1000$ the modulation of the unseeded laser pulse [Fig. 6(a)] is small, and the wake field [Fig. 8(a)] at this time is still almost all noise and very low in strength. Both the time for modulation of the laser pulse, and for clean wake field production is greatly reduced. A comparison of the spectrum at $\omega_p t=1000$ again shows little Raman energy in the unseeded [Fig. 7(a)] laser pulse as expected. However, in the plasmon [Fig. 7(b)] seeded and Raman [Fig. 7(c)] seeded laser pulses there is considerable Raman energy in the first and higher order shifts. These higher order Raman shifts will not produce reso-

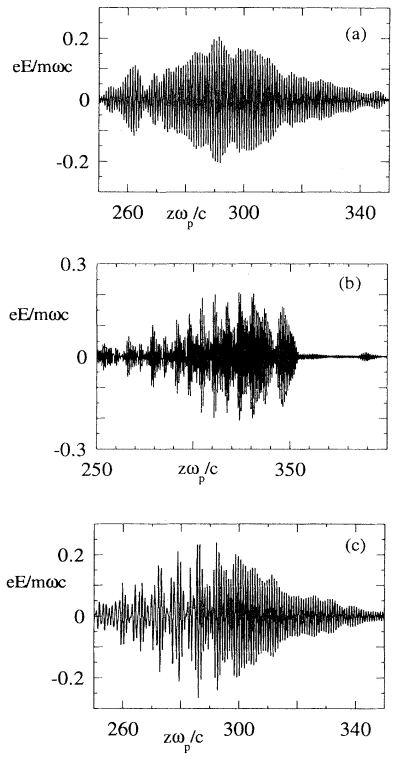

FIG. 3. (a), (b), and (c) show the unseeded, shaped, and Raman seeded laser pulses at $\omega_p t=750$.

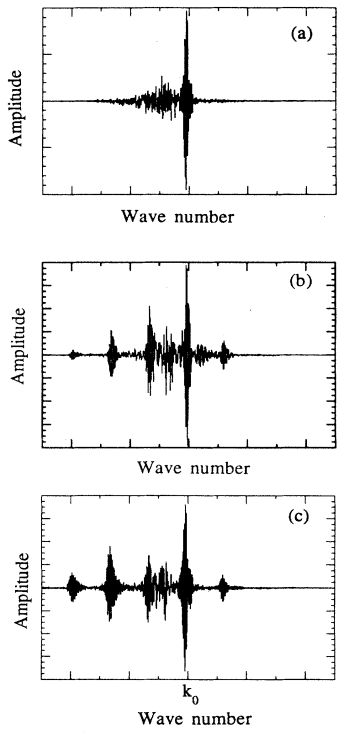

FIG. 4. (a), (b), and (c) show the unseeded, shaped, and Raman seeded wave-number spectra at $\omega_p t=750$.

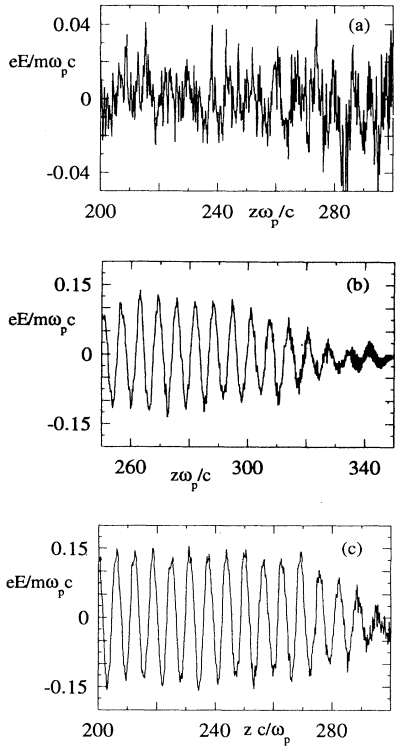

FIG. 5. (a), (b), and (c) show the wakefield induced by the unseeded, shaped, and Raman seeded laser pulses. $\omega_p t = 750$.

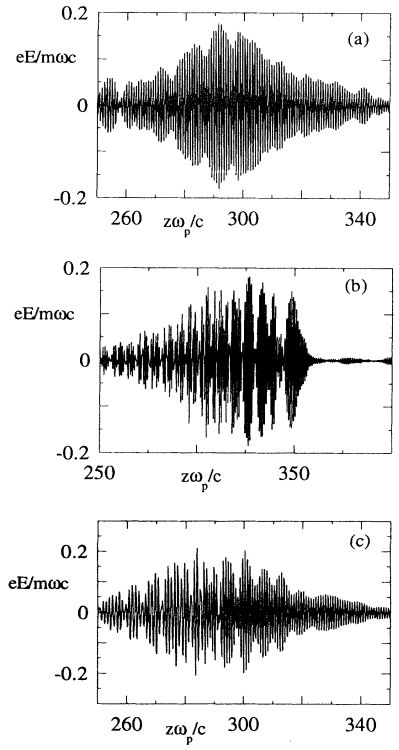

FIG. 6. (a), (b) and (c) show the unseeded, shaped, and Raman seed laser pulses at $\omega_p t = 1000$.

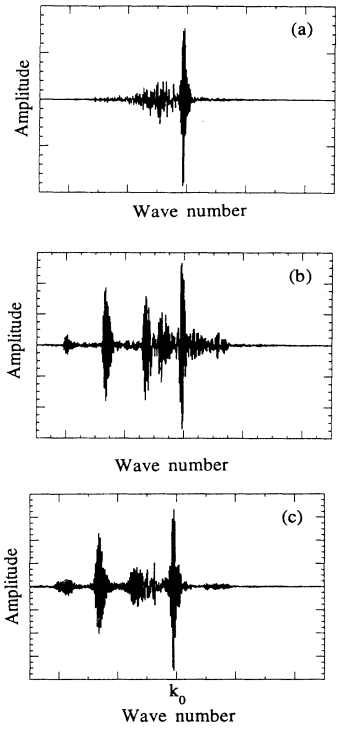

FIG. 7. (a), (b), and (c) show the unseeded, shaped, and Raman seeded wave-number spectra at $\omega_p t = 1000$.

nant ponderomotive kicks for the plasma oscillations when beating with the original laser radiation, and this accounts for the degradation of the wake field for the plasmon seeded [Fig. 8(b)] and for the Raman seeded [Fig. 8(c)] laser pulses. These higher order Raman shifts may be seen in the laser pulses as spikes between the resonant spikes (resonant spikes are λ_p apart).

V. SEED PRODUCTION

There are two basic ways to produce the Raman seed pulse for the laser pulse; the first is to separate some of the original laser pulse, and shift that pulse (or part of it) to the desired frequency by using a plasma or some other parametric process. The second is to self-seed the laser pulse itself, which could be accomplished by using RFS or some other nonlinear process. Since only the first shifts are usually wanted (higher order are unwanted as they are usually destructive to the wakefield), the higher order could be removed by a mirror reflective to only the wanted frequencies or by spatial filtering of the spectrum. If multiple orders are properly phased and have certain amplitudes, they may produce sharper and more intense laser spikes for greater amplitude wake fields. Also, if preseeding is used, the laser pulse would also remove any sidescatter, which would interfere and dirty the modulation of the laser pulse and the wake field.

One method would be to focus the laser multiple times into the plasma [14]. Each time the amount of Raman energy would grow, and while the pulse is outside the focus unwanted order energy shifts could be removed. Also, the desired Raman energy could be separated from

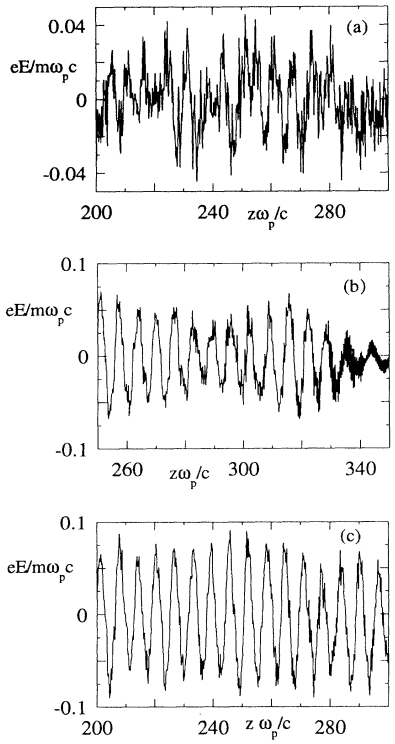

FIG. 8. (a), (b), and (c) show the wakefield induced by the unseeded, shaped, and Raman seeded laser pulses. $\omega_p t = 1000$.

the laser pulse and recombined to produce a better distribution of seeded energy within the laser pulse. An alternate method would be to use some nonlinear optical process (optical parametric process, atomic Raman, etc.) to produce the seed. This should not be difficult as only a small amount of the original energy need be converted depending upon the parameters (approximately 0.1% typical).

The plasmon seed may be produced by the laser pulse that is to be modulated, or the plamsa oscillation may be produced before the laser pulse arrives. This initial plasma oscillation may be induced by any process (laser pulse, particle beam, etc.).

VI. APPLICATIONS AND CONCLUSION

We see as applications for SRFS the production of very short high intensity laser pulses and electron beams, in addition to the obvious application in laser wake-field acceleration that has already been discussed in the previous sections. When a substantial amount of energy from the original laser pulse has been converted into the Raman forward scattered radiation, simulations show that the original pulse has been chopped into short intense (as energy is compressed into these short pulses) laser pulses. The length and separation of these short laser pulses is adjustable by varying the density and into which Raman order the energy flows. When the majority of the shifted energy is in the first order, the short chopped laser pulses will have a length of λ_p. If in the second order, the laser pulses will have a length of $\lambda_p/2$, and so forth. The energy flow for each other progresses from that order to the next order (for example from first to second). These short pulses may be separated and used for any general purpose or as a train of short laser pulses. The length of this train depends on the length of the original laser pulse used to make the train.

The production of very short electron beams is accomplished by putting to use the strong wake field induced by the Raman modulated laser pulse. This wakefield may be used to bunch an injected long electron beam or produce bunches from those plasma electrons accelerated by the wake field. Bunching of the electron beam is accomplished by the alternating accelerating and decelerating regions of the wake field, causing the electrons to bunch into the region of acceleration. These bunches are short ($\approx c/\omega_p$), and the spacing is λ_p, which are adjustable by varying the density. These bunches may be separated or used as a train of short electron bunches. An application of such ultrashort bunches to the generation of coherent x rays has been suggested [15]. Simulations have shown that with a shaped or intensity seeded laser pulse, the time for significant SRFS to occur can be drastically reduced accompanied with the production of a cleaner wake field.

Using a seeded laser pulse may be a cheap and easy method to produce high energy electrons. The reproducibility should be good as long as the seed source and laser pulse have good reproducible characteristics. A seeded low intensity laser pulse may be used in a high density plasma to form very strong wake fields, making a relatively inexpensive accelerator. Without seeding, the time for a lower intensity laser pulse to modulate could be long, much longer than the interaction length, and in this case pulse modulation would never occur.

Seeding is especially important in certain regimes where the growth rate for SRFS is low. These regimes include when the plasma density is low, the laser intensity is low, or both. It is also important when the laser pulse is short (but still longer than λ_p).

ACKNOWLEDGMENTS

This work was supported by the U.S. Department of Energy. We would also like to thank M. Downer, C. W. Siders, and K. Nakajima for useful discussions.

[1] K. Nakajima *et al.*, Phys. Rev. Lett. **74**, 4428 (1995).
[2] T. Tajima and J. M. Dawson, Phys. Rev. Lett. **43**, 267 (1979).
[3] P. Sprangle, E. Esarey, A. Ting, and G. Joyce, Appl. Phys. Lett. **53**, 2146 (1988).
[4] C. Joshi, T. Tajima, J. M. Dawson, H. A. Badis, and N. A. Ebrahim, Phys. Rev. Lett. **47**, 1285 (1981).
[5] N. E. Andreev, L. M. Gorbunov, V. I. Kirsanov, A. A. Pogosova, and R. R. Ramazashvili, Pis'ma Zh. Eksp. Teor. Fiz. **55**, 551, (1992) [JETP Lett. **55**, 571 (1992)].
[6] J. Krall, A. Ting, E. Esarey, and P. Sprangle, Phys. Rev. E **48**, 2157 (1993).

[7] William L. Kruer, *The Physics of Laser Plasma Interactions* (Addison-Wesley, Reading, MA, 1988).
[8] T. Tajima, Laser Part. Beams **3**, 351 (1985).
[9] E. Esarey, G. Joyce, and P. Sprangle, Phys. Rev. A **44**, 3908 (1991).
[10] E. Esarey, J. Krall, and P. Sprangle, Phys. Rev. Lett. **72**, 2887 (1994).
[11] B.N. Breizman, T. Tajima, D. L. Fisher, and P. Z. Chebotaev, in *Research Trends in Physics: Coherent Radiation Generation and Particle Acceleration,* edited by A. M. Prokhorov (AIP, New York, 1992).
[12] D. H. Reitze, A. M. Weiner and D. E. Leaird, Appl. Phys. Lett. **61**, 1256 (1992).
[13] A. M. Weiner *et al.*, IEEE J. Quantum Electron. **28**, 908 (1992).
[14] D. Umstadter, E. Esarey, and J. Kim, Phys. Rev. Lett. **72**, 1224 (1994).
[15] A. Ogata and K. Nakajima (unpublished).